Forest Ecology and Management 606 (2026) 123568

Contents lists available at ScienceDirect

Forest Ecology and Management

journal homepage: www.elsevier.com/locate/foreco

The climate-fire nexus: Understanding post-fire vegetation recovery

Fernando Pérez-Cabello *, Roberto Serrano-Notivoli, Raquel Montorio, Cristian Iranzo

Departamento de Geografía y Ordenación del Territorio, Instituto Universitario en Ciencias Ambientales de Aragón (IUCA), Universidad de Zaragoza, Zaragoza, Spain

ARTICLE INFO

Keywords:
Post-fire regeneration
Mediterranean forests
Burn severity
Remote sensing
Leaf area index (LAI)
Generalized linear mixed models (GLMM)

ABSTRACT

In Mediterranean ecosystems, high-frequency hydroclimatic variability, along with shifts in the fire regime, are key drivers of forest degradation. In this context, understanding post-fire vegetation recovery is crucial for both ecological research and forest management standpoint. Satellite-based remote sensing, particularly through orbital platforms, provides a robust framework for tracking post-fire vegetation dynamics. We assessed recovery patterns across 30 fire-affected areas in Aragón (northeastern Spain) by analyzing temporal trends in the Leaf Area Index (LAI), a widely used proxy for canopy structure, primary productivity, and vegetation health. Using Generalized Linear Mixed Models (GLMMs), we modeled LAI trajectories as a function of fire severity, dominant plant regenerative traits, and post-fire climatic conditions (drought or wet periods), including fire location as a random effect to account for spatial heterogeneity among burn sites. The models showed strong predictive capacity ($R^2 \approx 0.80$), and the inclusion of random effects substantially improved model fit, underscoring the importance of site-specific factors in shaping recovery dynamics. Fire severity and post-fire moisture availability—particularly during the first years—were the most influential drivers of LAI regeneration. The regeneration mechanism of dominant vegetation also contributed to early post-fire recovery, although its influence diminished over time. From a forest management perspective, these findings can inform the design of post-fire recovery strategies based on different post-fire moisture and severity conditions.

1. Introduction

Fire is one of the main natural factors shaping forest landscapes (Karavani et al., 2018; Keeley et al., 2011; Pausas and Keeley, 2009; Pyne, 2007; Rundel et al., 2016). Fire regimes influence the structure, species composition, adaptive traits of plant species, and biogeochemical cycles of affected forest ecosystems (Pausas and Bond, 2020; Bond et al., 2005; Bond and Keeley, 2005). However, wildfires have become a major issue in regions such as southern Europe due to disruptions in their natural regimes in the 21st century (Kapsomenakis et al., 2023; Pausas and Fernández-Muñoz, 2012; Lloret, 2004). Fuel accumulation resulting from the abandonment of traditional land-use practices, together with the increased frequency of extreme drought events associated with persistent dry atmospheric conditions, are the main drivers behind the rising occurrence, extent and intensity of wildfires (McClure et al., 2024; Fernández-García et al., 2019; Doblas-Miranda et al., 2017).

Fire affects all ecosystem components, but vegetation combustion and/or dehydration is its most immediate and ecologically significant consequence. At the ecophysiological level, foliage loss reduces photosynthetic potential and carbon sequestration capacity, while also altering the hydrological cycle by reducing transpiration and rainfall interception. These changes lead to multiple modifications in ecosystem-level interactions (Zhu et al., 2020). However, due to the effectiveness of vegetative regeneration mechanisms—such as resprouting from protected buds or lignotubers—vegetation recovery can begin shortly after the fire event in resprouting species, whereas seed-based regeneration usually occurs later, depending on post-fire rainfall and seed viability (Pausas and Keeley, 2014; Clarke et al., 2013).

Several previous studies analyzed post-fire response and monitored regeneration processes at different spatial scales. At the experimental plot scale, vegetation regeneration was typically assessed using parameters related to cover level, structure, and floristic composition (Moya et al., 2018; Baeza and Vallejo, 2008; Alvarez et al., 2005; Tárrega et al., 2001; Caturla et al., 2000; Garcia-Villanueva et al., 1998; Kazanis and Arianoutsou, 1996). However, when regional-scale assessments were required, field plot data had limited representativeness relative to the total affected area (Meng et al., 2015). In this context, orbital remote sensing data provided a widely recognized and valuable complement, given the sensitivity of spectral information in detecting fire-affected phenomena and the versatility of remote sensing products. These data

* Corresponding author.
E-mail address: fcabello@unizar.es (F. Pérez-Cabello).

https://doi.org/10.1016/j.foreco.2026.123568
Received 16 August 2025; Received in revised form 21 January 2026; Accepted 24 January 2026
Available online 30 January 2026

enabled the monitoring of areas of varying extents over time (Desrochers et al., 2025; Woodgate et al., 2025; Marcos et al., 2023; Meneses, 2021; Gitas et al., 2012; Lentile et al., 2006).

From an operational perspective, Landsat satellite imagery combined with spectral indices based on differences between red and near-infrared reflectance, is one of the most commonly used approaches (Borini Alves et al., 2015; Vicente-Serrano et al., 2011). In contrast, the use of more complex biophysical parameters, also derived from spectral information, is less frequent. These include the Leaf Area Index (LAI) and the fraction of Absorbed Photosynthetically Active Radiation (fPAR). LAI is a structural canopy property defined as the photosynthetically active leaf surface area per unit of ground area (Chen and Black, 1992). It serves as a bioindicator of plant health and gross primary productivity (Fang et al., 2019), and it is widely used in models to simulate productivity and CO_2 storage (Pu et al., 2020; Rajib et al., 2020; Ling et al., 2019). Therefore, it could also be a key parameter for assessing foliar regeneration and, consequently, the recovery of the eco-physiological functioning of fire-affected areas (Zang et al., 2025).

The MODIS (Moderate Resolution Imaging Spectroradiometer) sensor is one of the most widely used orbital systems for monitoring land surface changes due to its spatial and spectral characteristics (Ganguly et al., 2012; Justice et al., 2002). In addition to capturing images across 19 discrete optical bands (ranging from 0.4 to 2.5 μm), MODIS provides various products specifically designed to study biophysical variables such as LAI, fPAR, and GPP, which can be used to better understand vegetation regeneration processes in burned areas (Jiménez Ruano et al., 2016). The primary algorithm for deriving LAI is based on a 3D radiative transfer model (Knyazikhin et al., 1998), which is inverted using a Look-Up Table (LUT) specifically designed for different biome types on a global scale. It also incorporates other products, such as adjusted reflectances, leaf optical properties, and ancillary information sources (e.g., ecosystem type maps). This higher level of processing complexity—taking into account how light interacts with leaves, soil, and other elements—provides more detailed information than the direct observation of reflectance in different spectral bands.

The availability of LAI data series at different temporal scales in large fire-affected areas allows the analysis of how natural and anthropogenic factors, both structural and contingent, influence the observed trends. Structural factors refer to inherent environmental characteristics (e.g., topography, lithology, climate, vegetation), where the regeneration mechanism of the affected species stands out, characterized by a strong prevalence of resprouting and germination mechanisms in fire-adapted ecosystems (Pausas and Vallejo, 1999). Contingent factors are those whose influence is limited to specific post-fire periods or events (e.g., implementation of hydrological-forestry restoration measures, thermal-precipitation anomalies in the year of the fire and subsequent years, or burn severity).

Although the role of burn severity [i.e., the level of damage caused by fire, expressed in terms of the magnitude of ecological change (Key and Benson, 2006)] is of paramount importance, there are still some uncertainties regarding how post-fire responses vary with burn severity. High severity is generally associated with greater burning of vegetation cover and increased soil alteration (Alcañiz et al., 2018; Moody et al., 2013; Neary et al., 2005; Shakesby and Doerr, 2006).

Previous studies have highlighted the importance of post-fire climatic conditions and identified them as one of the key factors explaining vegetation recovery (Celebrezze et al., 2024; Viana-Soto et al., 2020; Bright et al., 2019; Meng et al., 2015; Smith-Tripp et al., 2026).

While the influence of water availability and drought on vegetation recovery and LAI dynamics after fire has been examined in several studies (Shi et al., 2025), fewer works have explicitly assessed this relationship across multiple vegetation types and fire severity conditions using a spatially explicit, long-term remote sensing approach.

Sufficient moisture availability after a fire is crucial for seed germination (Tappeiner et al., 1992), but drought can limit seedling establishment and growth (Crockett and Hurteau, 2024; Lalor et al., 2023; Daskalakou and Thanos, 2004; Donato et al., 2009). The timing of these anomalies in water resources following a fire is also critical in determining their impact on ecosystem regeneration, as their influence may be particularly significant in the early post-fire stages and diminish over longer periods, or they may persist as a consistently relevant factor over time (Stevens-Rumann and Morgan, 2019; Harvey et al., (2016). For this reason, the Standardized Precipitation and Evapotranspiration Index (SPEI) (Vicente-Serrano et al., 2010) is a useful indicator of climatic conditions for vegetation recovery since it reliably estimates the available moisture at different aggregated time scales, when the impacts on vegetative activity may vary.

Based on these assumptions, research questions arise: How do burn severity and post-fire moisture conditions (i.e., rainfall and drought patterns) influence the regenerative dynamics of vegetation in Mediterranean environments? What role do species regeneration mechanisms play in the recovery of the LAI after fire, and how does their impact change over time? How do local environmental conditions influence post-fire vegetation recovery, and to what extent do they contribute to variations in LAI trends?

This study aims to evaluate the recovery of foliage status, represented by the LAI trends at different post-fire time scales (from 1 to 5 years), by analyzing the explanatory capacity of: 1) post-fire climatic conditions, assessed using SPEI over time windows matching the LAI trends; 2) burn severity, and 3) dominant regeneration mechanism of the affected vegetation types. Variables (2) and (3) are derived from Landsat products, while LAI trends are obtained from MODIS data at a moderate spatial resolution (500 m). To reconcile the difference in spatial resolution between the datasets, Landsat-derived variables were spatially aggregated by computing central tendency measures within the MODIS pixel extent, allowing for consistent integration of fine-scale explanatory variables with moderate-resolution LAI dynamics.

We focus on 30 areas affected by wildfires (2003–2015) in the region of Aragón (northeastern Spain), using Generalized Linear Mixed Models (GLMM) to incorporate fixed and random factors to identify their distinct roles in post-fire vegetation recovery. Between 2001 and 2022, a series of fire events in Aragón resulted in the loss of more than 70,000 ha, leading to the alteration of large areas, particularly affecting sclerophyllous and sub-sclerophyllous shrub and tree plant communities.

This study addresses the need for diagnostic methods and monitoring protocols in burned areas to assess post-fire vegetation response. From a forest management perspective, it offers insights for planning hydrological-forestry interventions under varying climatic scenarios to improve ecosystem management and conservation.

2. Methods

The methodology applied in this study is structured into six main stages, which are summarized in Fig. 1. First, (1) fire-affected areas are selected and mapped. Next, (2) the regenerative trend (*T-LAI*) is generated using the MCD15A2Hv061 product. This is followed by (3) a post-fire climate characterization through the SPEI, (4) a spatial analysis of burn severity, and (5) an analysis of pre-fire vegetation with aggregation based on regeneration mechanism. Finally, (6) a post-fire recovery modeling is conducted.

2.1. Selection of fire-affected areas

The first phase involved the identification and mapping of fires in Aragón that occurred between 2003 and 2015. This time frame was selected based on the availability of the MODIS LAI product (MCD15A2Hv061) and the objective of monitoring post-fire dynamics over five years following each fire. Due to the different spatial scales of the variables integrated into this study, the analysis was limited to burned areas larger than 100 ha to ensure the largest number of observations free from potential contamination by unburned areas. To this

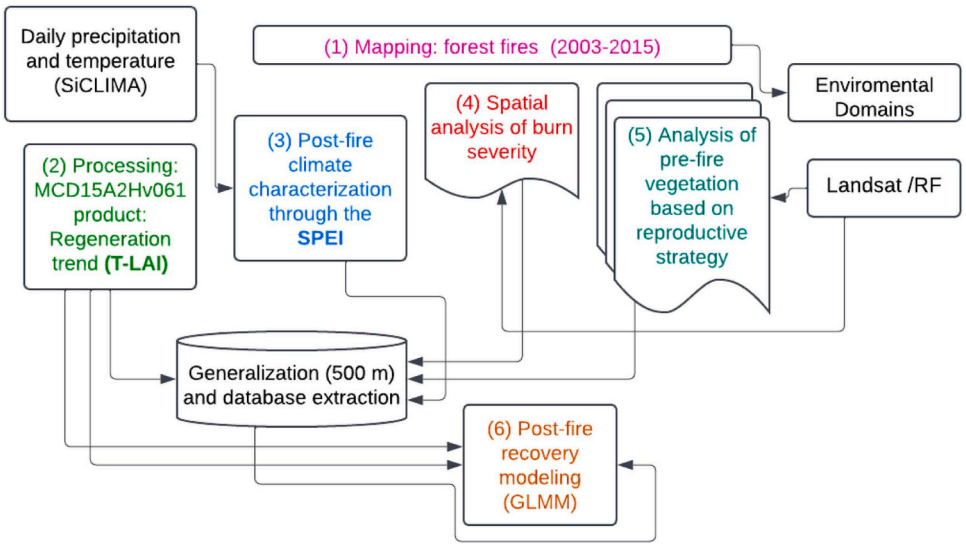

Fig. 1. Workflow followed to assess post-fire vegetation recovery. SiCLIMA: *High-resolution hydroclimate and temperature dataset for Aragón (northeast Spain)* (Serrano-Notivoli et al., 2024); SPEI: *Standardized Precipitation and Evapotranspiration Index*; T-LAI: *Trend of the Leaf Area Index (LAI) from MODIS (MCD15A2Hv061)*; GLMM: *Generalized Linear Mixed Models*. RF: *Random Forest*.

end, we used the fire database from the Government of Aragón.

A total of 30 fire perimeters (mean size 1285 ha; ranging from 103 to 6382 ha), distributed throughout the forested areas of Aragón, were selected (Table S1 and Fig. 2). These fires were grouped into three environmental domains:

1. Mid-elevation (500–775 m) (8 fires). Areas with a continental Mediterranean climate, characterized by an average annual temperature between 12 °C and 14 °C and precipitation ranging from 500 to 600 mm. These fires are located mainly in the mid-mountain areas of the *Sistema Ibérico* (Iberian System), within the mesomediterranean belt, with a dry to sub-humid climate. The dominant vegetation

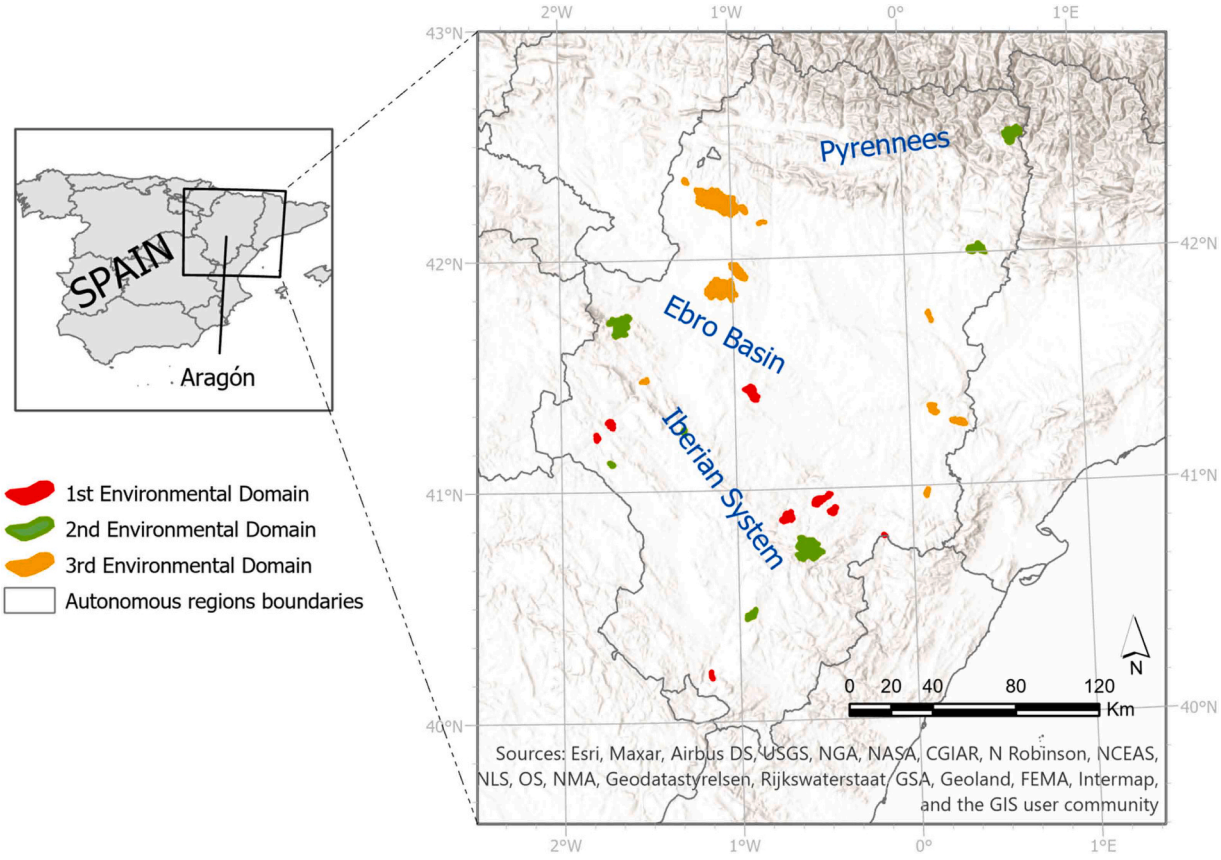

Fig. 2. Areas affected by fire depending on the type of aggregation domain. *Not all individual fire perimeters may be visible (either because they are small or because they overlap)*.

belongs to the holm oak series (*Quercetea ilicis*), which is typical of inland Mediterranean areas with moderate continentality.

2. High-elevation (> 1000 m) (7 fires). These areas have a sub-Mediterranean climate with an average annual temperature between 10 °C and 12 °C and annual precipitation exceeding 700 mm. This area encompasses the highest elevations of the Pyrenean and Iberian mountain ranges. The dominant climax vegetation consists of deciduous oak forests (*Quercus faginea* L., *Quercus pubescens* Willd., and *Quercus cerrioides* Willk. & Costa), while *Buxus sempervirens* L., *Genista scorpius* (l.) DC. and *Echinospartum horridum* (Vahl) Rothm. shrublands appear as secondary vegetation. At the highest elevation, mountain pine forests of *Pinus sylvestris* L. predominate. According to the phytoclimatic classification, this domain falls within the montane-supramediterranean belt, with a sub-humid climate, and belongs to the *Quercetea pubescentis* vegetation series, typical of mountainous areas with higher relative moisture.
3. Low-elevation (< 500 m) (15 fires). Mainly distributed across lowlands of the Ebro Basin and the Iberian and Pyrenean foothills, on Tertiary and Quaternary substrates. This region is characterized by a semi-arid Mediterranean climate, with average annual temperatures ranging from 14 °C to 16 °C and low annual precipitation (~450 mm). According to Rivas-Martínez's phytoclimatic classification, this area belongs to the mesomediterranean belt with a dry to semi-arid climate (Rivas-Martínez et al., 2002). The dominant vegetation includes kermes oak (*Quercus coccifera* L.) and holm oak (*Quercus. ilex* L.) shrublands, although *Pinus halepensis* L. woodlands are also abundant, accompanied by *Q. coccifera* L. and other characteristic Mediterranean shrub species.

2.2. Generation of the regenerative trends ($T\text{-}LAI$ and $T\text{-}LAI_C$)

MODIS data were obtained from the *Land Processes Distributed Active Archive Center* (LPDAAC). The MCD15A2Hv061 LAI product has a spatial resolution of 500 m and an 8-day temporal resolution. Although field-based LAI validation data were not available for the study area, the MODIS LAI/FPAR (MCD15A2H) product has been extensively validated through comparisons with in-situ measurements and independent satellite datasets (Morisette et al., 2006; Garrigues et al., 2008). While some studies have reported a slight overestimation of MODIS LAI values (Yan et al., 2016), these products have been shown to reliably capture vegetation phenological dynamics and temporal trajectories (Serbin et al., 2013). More recent evaluations report an acceptable agreement between MODIS LAI and reference data ($R^2 \approx 0.7$; RMSE ≈ 0.96; Lin et al., 2023).

All pixels classified as burned (dNBR > 100, following the official threshold distinguishing burned from unburned areas; see 2.4) that intersected fire perimeters between 2003 and 2015 were selected, yielding a total of 1605 burned pixels. In addition, a control group was defined using 878 pixels located within or adjacent to fire perimeters but showing dNBR values < 100, ensuring that these pixels had not been affected by fire.

From both datasets (burned and unburned or control), we computed two LAI trends ($T\text{-}LAI$ *and* $T\text{-}LAI_C$) after fire occurrence for all pixels over five periods (1–5 years) —a common time-frame choice in similar studies to assess short-term regeneration (Meng et al., 2015; Carlson et al., 1990). Both trends were analyzed using approximately 228 observations, allowing for the estimation of both the statistical significance using the Mann-Kendall statistical test (Kendall, 1975) and the magnitude of the trend using Sen's slope estimator (Sen, 1968). Since LAI data exhibited a pronounced seasonality due to the natural cycles of vegetation growth and senescence, they were deseasonalized before calculating the trends. The STL (Seasonal-Trend decomposition using Loess) approach (Cleveland et al., 1990) was used to isolate the underlying long-term trend, providing a clearer view of significant changes over time.

2.3. Post-fire climate characterization through the SPEI

The SPEI is obtained by normalizing the water balance to the log-logistic probability distribution (Vicente-Serrano et al., 2017). Its main advantage over other drought indices is that it takes into account the concurrence of precipitation and temperature, making it a useful tool to assess soil water availability. In addition, it allows the association of different drought temporal scales with specific events such as wildfires (Russo et al., 2017; Vicente-Serrano et al., 2010). The SPEI quantifies data anomalies based on the number of standard deviations by which the value deviates the long-term hydroclimatic mean for a specific location (i.e., when SPEI > 1, it indicates an anomalously wet period; when SPEI < −1, it indicates an anomalously dry period).

Drought intensity values obtained through the SPEI were calculated using the SiCLIMA dataset (Serrano-Notivoli et al., 2024), a 0.25 km^2 (500 ×500 m) grid of daily precipitation and temperature data covering the Aragón region. This dataset was built from more than 3000 observational data series of both variables, which underwent comprehensive quality control and reconstruction. The latter was performed by estimating values at unmeasured locations using generalized linear models (GLM and GLMM) and incorporating environmental and topographic variables as predictors independently for each day and location.

2.4. Spatial analysis of burn severity

The analysis of burn severity using multispectral remote sensing (Landsat imagery) was based on its ability to detect changes in surface reflectance caused by vegetation loss, increased soil exposure, variations in moisture content, or the appearance of combustion-derived substances. One of the most effective spectral indices for this purpose is the Normalized Burn Ratio (NBR) (Epting et al., 2005), as it combines the spectral bands that show the strongest contrast in response to fire: near-infrared (NIR) and shortwave infrared (SWIR). NIR shows a decrease in reflectance due to the loss of active vegetation, while SWIR registers an increase in reflectance due to moisture loss and greater soil exposure (Van Wagtendonk et al., 2004).

The NBR index is generally applied in a bi-temporal approach using pre- and post-fire data, which results in the delta Normalized Burn Ratio (dNBR) (Key and Benson, 2006) and the Relative delta Normalized Burn Ratio (RdNBR) (Miller and Thode, 2007). Both bi-temporal indices can be calculated to obtain an initial assessment of burn severity, typically using a post-fire image acquired shortly after the fire event (Cocke et al., 2005; French et al., 2008; Parks et al., 2019; Saberi et al., 2022). However, RdNBR eliminates the bias associated with pre-fire vegetation conditions by normalizing dNBR to the pre-fire NBR value.

2.5. Analysis of pre-fire vegetation and aggregation based on regeneration mechanism

To characterize pre-fire vegetation and its spatial distribution, mapping products were generated to identify the dominant plant communities affected by fire. This classification was not intended to represent discrete ecological units at the species level, but rather to provide an ecologically meaningful framework for aggregating vegetation according to dominant post-fire regeneration strategies, which are a key determinant of recovery dynamics in fire-prone ecosystems.

Multispectral satellite images from the Landsat program, available in the Google Earth Engine (GEE) repository at Level 2 processing (Collection 2), were used for this purpose. A composite image was generated for each year, based on the median surface reflectance values from available images acquired between June and October, filtered by cloud mask cover and with cloudy pixels removed using a cloud mask (Schmitt et al., 2019). A supervised classification algorithm based on Random Forest (RF) was then applied. The training process was conducted using a field database containing 3100 labeled samples from 2013, developed within the framework of previous research projects and

various cartographic sources of forest information, in particular the Third National Forest Inventory (NFI-3).

A total of eight vegetation categories were obtained, distributed across four tree vegetation types [*Pinus sylvestris* (Ps), *Pinus nigra* (Pn), *Quercus ilex* (Qi), and *Quercus cerrioides* (Qf)], three shrubland types [shrublands derived from *P. sylvestris* (mPs), shrublands derived from *Q. cerrioides* (mQf) –i.e., shrublands colonizing fire-affected *P. sylvestris or Q. cerrioides* stands–, and degraded low shrublands (mP)], and one category representing areas with sparse or no vegetation (I).

Regeneration mechanisms were not directly derived from Landsat imagery but were assigned a posteriori based on the dominant vegetation types identified through the supervised classification. This assignment was grounded in well-established fire-response traits documented in the ecological literature (e.g., Pausas et al., 2004), reflecting species-level strategies related to fire resistance, resprouting capacity, and recruitment from seed.

Broadly, the ecosystems included in the study represent three dominant post-fire regeneration strategies: (a) obligate seeders, dominated by *P. halepensis*, a species with an extensive aerial seed bank (serotiny) that allows endogenous recolonization; (b) passive defense systems, characteristic of communities dominated by *P. nigra* and *P. sylvestris*, which adopt a fire-resistant strategy through passive defense mechanisms (e.g., relatively thick bark or high crown base height); and (c) obligate resprouters, represented by phanerophytes and macrophanerophytes of the genus *Quercus* (*Q. ilex*, *Q. cerrioides*, *Q. coccifera*), which rely on resprouting from adventitious buds. Although shrub communities may exhibit heterogeneous post-fire regeneration strategies, limitations in the spectral discrimination of shrub species using Landsat imagery required their aggregation into a single category. This functional grouping is appropriate at regional scales and when using medium-resolution satellite-derived indicators such as LAI, where species-level variability cannot be resolved but dominant ecological strategies governing post-fire recovery can be robustly captured.

2.6. Statistical analysis and post-fire recovery modeling

We used Generalized Linear Mixed Models (GLMM) to assess the effect of climatic constraints on LAI trends, while controlling for burn severity and the characteristics of the affected vegetation.

Five different models were computed for the five cumulative time periods considered in the τ-LAI from 1 to 5 years after fire occurrence (+12, +24, +36, +48, and +60 months). As GLMM allow for the adjustment of correlation structures that include fixed effects (explanatory variables) and random effects (variables that account for unexplained variability) (Bolker et al., 2009), we included the SPEI variables at different temporal scales, short-term burn severity and occupancy percentages based on regeneration mechanism as fixed effects, while the location of the fires (their individual identifier) was the random effect.

In addition, to identify whether the LAI trend in burned areas responds exclusively to climatic variations (common across the entire landscape –burned and control) or reflects a specific postfire regeneration process modulated by fire impact and the functional traits of the vegetation, a second set of models was computed including the interaction between SPEI and the burned-control categories.

In both cases, the model parameters were estimated using the restricted maximum likelihood (REML) method, and the variables were previously standardized to ensure comparability of coefficient magnitudes, improve convergence (achieving a stable solution after a defined number of iterations), and enhance the model's numerical stability.

Before applying the models, we partitioned the input data into two groups, of which one (30 %) was reserved for testing purposes and the other (70 %) was used as training dataset. We performed 10,000 realizations to avoid bias in the selection of data and the results were averaged.

In addition, to evaluate differences in LAI among the different Domains, the non-parametric Kruskal–Wallis test was applied, followed by pairwise comparisons using the Steel–Dwass–Critchlow–Fligner post-hoc test. Likewise, differences in LAI between burned and control areas were assessed using the Wilcoxon signed-rank test for paired samples, applied at 100-day post-fire intervals to capture temporal recovery patterns. Prior to the analyses, a stratified random sampling procedure was implemented to minimize pseudo-replication and ensure the spatial independence of observations. Specifically, 100 pixels per Domain were selected for the Kruskal–Wallis test. For the Wilcoxon test, a Monte Carlo approach was applied for each 100-day interval (18 in total), performing 100 iterations consisting of the random selection of 300 observations from each sample (burned and unburned).

3. Results

3.1. LAI-based fire clustering

The three environmental domains derived from the clustering of the 30 fire events were dominated by Mediterranean and sub-Mediterranean pine forests with deciduous and evergreen oaks, and they were representative of a climatic-altitudinal gradient, with changes in the leaf fraction and the regenerative strategy of the dominant tree species (Table 1).

Fires in the foothills of the Iberian System and the Ebro Basin (LAI: 0.57, ALT: 750 m) (Domain 1st) featured plant communities with low foliar density, corresponding to open or degraded forests, dominated by shrubs and tree stands of *Pinus halepensis* (10.84 %). The fires in the mid-elevation Pyrenees and Iberian System (LAI: 0.86, ALT: 1200 m) (Domain 2nd) showed the highest values, representing denser vegetation types with high foliar density. These areas were dominated by *Pinus sylvestris/nigra* (21.83 %), with a significant contribution from marcescent and evergreen broadleaved species-*Quercus faginea/Quercus ilex* (10.04 %).

Finally, fires in the Ebro Basin and the Pyrenean Piedmont (LAI: 0.70, ALT: 537 m) (Domain 3rd) presented an intermediate LAI, suggesting vegetation types with moderate foliar density, mainly composed of *Pinus halepensis* (2.19 %), with smaller contributions from *P. nigra* (4.24 %) and *Quercus gr. cerrioides/Quercus ilex* (1.97 %). Statistical analyses confirmed significant differences in LAI among domains, both before ($K = 28.82$, $p < 0.0001$) and after fire ($K = 67.30$, $p < 0.0001$). In both cases, Domain 1st had significantly lower LAI values than Domains 2nd and 3rd ($p < 0.05$), while no significant differences were detected between Domains 2nd and 3rd ($p > 0.05$).

3.2. Post-fire vegetation recovery trends (τ-LAI and τ-LAI$_C$)

The morphological characteristics of the probability density distributions across post-fire periods of different length (Fig. 3) allowed the identification of three τ-LAI patterns. The first one, corresponding to the initial 12 months after the fire, exhibited high variability with a notable presence of cases showing a negative trend. During the first 24 months after the fire, there was a period of high post-fire regeneration, characterized by predominantly positive trends. From 36–60 months after the fire, a prevalence of weak positive trends was observed, indicating a stabilization process. This was reflected in the reduction of skewness and kurtosis (Table 2), as well as in the convergence of distributions toward values close to zero, particularly after 48 months. Both patterns suggested that trends become less pronounced and more stable as longer post-fire periods are considered.

Obviously, given the method used to calculate τ-LAI (accumulating one year in each measurement), these values are highly correlated. In fact, all correlations were significant and positive, except for the τ-LAI of the first year, which showed a negative correlation of lower intensity compared to the others ($r < -0.55$) (Table S2). On the other hand, the mean trends in the control areas (τ-LAI$_C$) show lower values and smaller percentages that are statistically significant (Table S3).

Fig. 4 shows the deseasonalized trajectory of LAI in burned areas (red

Table 1
General characteristics of fire clusters (environmental domains). For each domain, the table reports total burned area (EXT, ha) and number of wildfires (in parentheses), mean ± SD of pre- and post-fire LAI, elevation (ALT, m), burn severity (RdNBR), and mean surface area (MSA, %) corresponding to dominant post-fire regeneration mechanisms. MSA represents the percentage of the burned surface within each domain associated with each regeneration strategy: obligate seeders (OS), passive defense systems (PDS), and obligate resprouters (OR). Different letters ([a] vs. b) indicate statistically significant differences according to post-hoc tests.

	EXT (n° fires)	Pre-fire LAI	Post-fire LAI	ALT (m)	RdNBR	MSA: OS	MSA: PDS	MSA: OR
1st	5147 (8)	0.5653 ± 0.19[a]	0.4788 ± 0.14[a]	750 ± 100	561 ± 223	10.84 ± 17.2	0 ± 0.03	0.63 ± 1.58
2nd	16104 (7)	0.8557 ± 0.45[b]	0.7655 ± 0.35[b]	1200 ± 268	499 ± 236	0.01 ± 0.08	21.83 ± 22.8	10.04 ± 12.23
3rd	17294 (15)	0.6961 ± 0.23[b]	0.6647 ± 0.22[b]	537 ± 55	461 ± 221	2.19 ± 7.84	4.24 ± 9.89	1.97 ± 5.25

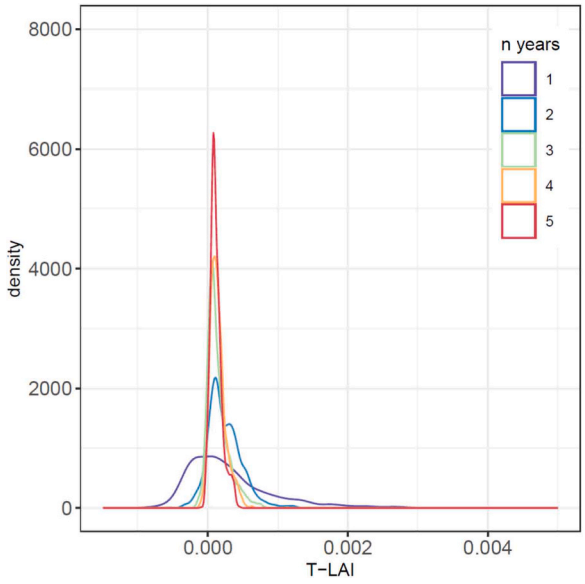

Fig. 3. Probability density distributions over post-fire time periods.

line) and control areas (green line) over a five-year period. In general, control areas exhibit consistently higher LAI values throughout the analyzed period. In contrast, burned areas show lower LAI values, not reaching the levels observed in non-affected areas until approximately three and a half years after the fire (p-value = 0.1005) (Table S4). Both groups show temporal fluctuations; however, the amplitude of variation is lower in burned areas, which may indicate a more limited vegetative response or a simplified vegetation structure in these sites.

3.3. Post-fire climatic conditions (SPEI)

The descriptive statistics for SPEI values at cumulative post-fire time steps (+12 to +60 months) are summarized in Table 3. This analysis follows a relative timeline, following a Superposed Epoch Analysis (Arizpe et al., 2020), where for each fire event (n = 30), SPEI values were extracted at specific intervals after the month of fire occurrence. As fire years differ (2003–2015), each time step refers to a distinct calendar period across fires. Therefore, the values presented do not correspond to a single climatic phase but instead reflect variability in post-fire drought exposure across events.

While no consistent pattern of extreme drought or wet conditions was observed across all time steps, certain periods (e.g., +36 months) showed broader ranges in SPEI values, including moderately to severely

Table 2
na.

Variable	Min.	Max.	Mean	Std. Dev.	Skewness	Kurtosis	% SIG
$T\text{-}LAI\_1st_{+12}$	-0.9074	1.0126	-0.1404	0.2882	0.3846	0.6946	84.05
$T\text{-}LAI\_2nd_{+24}$	-0.4989	1.2024	0.1199	0.1511	1.0396	5.1836	91.71
$T\text{-}LAI\_3rd_{+36}$	-0.2663	0.6494	0.0753	0.1114	1.3829	3.0813	89.35
$T\text{-}LAI\_4th_{+48}$	-0.1864	0.5895	0.0790	0.0834	1.0494	2.7001	95.20
$T\text{-}LAI\_5th_{+60}$	-0.1201	0.3655	0.0753	0.0636	0.9293	1.3294	96.26

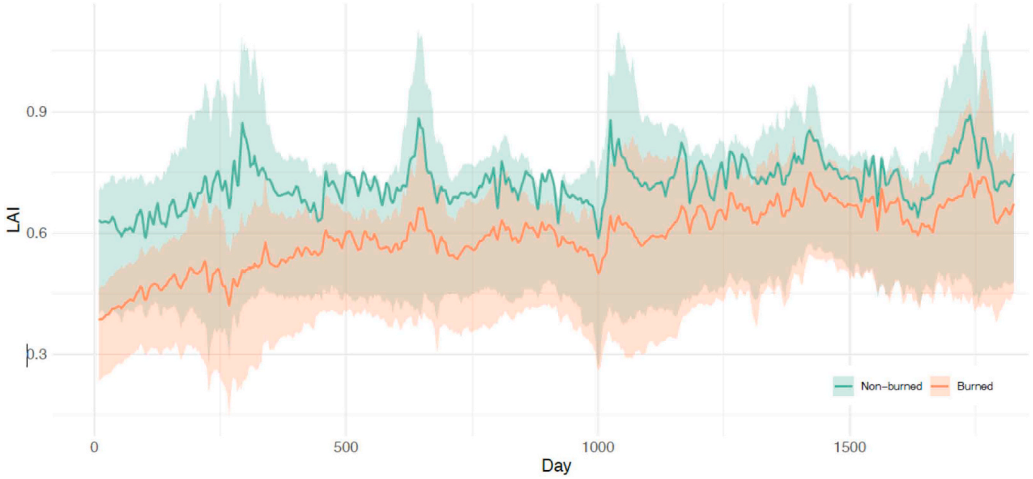

Fig. 4. Mean temporal evolution of LAI in burned and control areas over a five-year post-fire period. Shaded bands indicate the 5th–95th percentile range, illustrating the variability within each group.

Table 3
Distribution of descriptive statistics for SPEI values over 1–5 years post-fire cumulative time periods (+12 to +60 months).

Statistic	+ 12 m	+ 24 m	+ 36 m	+ 48 m	+ 60 m
Minimum	-1.2249	-1.3569	-1.3843	-1.7360	-1.5962
Maximum	1.5107	1.7418	1.8731	1.5699	1.5382
1st Quartile	-0.1373	-0.4285	-1.1761	-0.0772	-0.3075
3rd Quartile	0.4140	0.4187	0.5004	0.9685	0.7104
Standard deviations	0.6120	0.7023	0.7657	0.7039	0.7740
Skewness	0.1623	0.4599	0.4891	-0.5504	0.1451
Kurtosis	0.4980	-0.0903	-0.6599	-0.4041	-0.3631

dry or wet events. This variability highlights the heterogeneous climatic contexts experienced by different fires during their recovery periods. Notably, no fire events coincided with extremely dry or extremely wet conditions (SPEI ≤ -2 or ≥ 2).

3.4. Explanatory factors of *T-LAI*

Pearson's coefficient of determination obtained by comparing the observed and predicted values of *T-LAI* (in the 10,000 realizations of each model) reflected a satisfactory level of agreement ($R^2 \sim 0.80$). The marginal and conditional R^2 values (Table 4) showed moderate average values for the marginal ones (meaning that only 20 % of the variability is explained by the fixed effects) and acceptable values for the conditional ones ($R^2 = 0.66$, mean value for the time periods). This indicated that a significant proportion of the variability was due to the random effect, as the models together explained approximately 65 % of the total variance. In other words, the differences between burned areas explained a considerable part of the variance, which was key to understanding the magnitude of the *T-LAI*. This pattern was common when the data came from diverse geographic locations, as these often exhibited hierarchical or nested structures.

Table 4
Summary of model fit for the 10,000 iterations in the five models (+12 to +60 months), comparing predicted data with observed data not used in model construction (30 % data holdout; n = 482). R^2 marginal: variance explained by fixed effects; R^2 conditional: variance explained by the full model (fixed + random effects).

	Time interval	Min.	Mean	Max.	Std. Dev.
R^2 Pearson	*+ 12 m*		0.795	0.847	0.015
		0.735			
	+ 24 m		0.801	0.856	0.021
		0.726			
	+ 36 m		0.822	0.876	0.017
		0.758			
	+ 48 m		0.791	0.869	0.020
		0.712			
	+ 60 m		0.761	0.834	0.021
		0.676			
R^2 conditional	*+ 12 m*		0.612	0.666	0.014
		0.561			
	+ 24 m		0.717	0.775	0.018
		0.666			
	+ 36 m		0.686	0.735	0.014
		0.639			
	+ 48 m		0.642	0.699	0.016
		0.588			
	+ 60 m		0.653	0.702	0.012
		0.610			
R^2 marginal	*+ 12 m*		0.172	0.200	0.008
		0.144			
	+ 24 m		0.138	0.177	0.011
		0.103			
	+ 36 m		0.214	0.261	0.012
		0.173			
	+ 48 m		0.241	0.295	0.014
		0.195			
	+ 60 m		0.279	0.326	0.012
		0.228			

The most influential factor during the first period was SPEI (Fig. 5). Its influence then decreased sharply and became negligible in the models after + 12 months post-fire, highlighting the moment when moisture conditions were most needed for recovery. On the other hand, burn severity had a negative effect on *T-LAI* values that persisted for longer periods after the fire. Regarding the type of vegetation affected, regardless of its regeneration mechanism, it initially showed a negative relationship with *T-LAI* values. However, from + 12 months post-fire onwards, this relationship gradually shifted, approaching zero as the time intervals increased, being more important in resprouting tree species or those with a passive regeneration mechanism than in seeders.

In general terms, *T-LAI* indicated that the initial impact of fire (negative RdNBR and positive SPEI) decreased over time, while the positive influence of species began after the first year post-fire. These results emphasize the structural nature of the "previous vegetation" factor and the more circumstantial factors represented by burn severity or climatic anomalies.

3.5. Explanatory factors of *T-LAI* including interaction between SPEI and burn severity

The models fitted using pixel samples from both burned and control areas, incorporating vegetation functional traits, the SPEI, and the interaction between SPEI and burn condition, revealed temporal variations in the relative importance of these predictors (Fig. 6). In particular, the interaction term was statistically significant in the first three post-fire intervals (+12, +24, and +36 months), although with differing magnitudes and implications depending on the SPEI time scale considered (Table 6).

At 12 months post-fire, both the main effect of SPEI and its interaction with burn condition were positive and statistically significant on *T-LAI* (0.23 and 0.05, respectively). This suggests that moisture conditions near the time of the fire favored post-fire recovery. In the same interval, functional traits also played a notable role: resprouters were positively associated with *T-LAI*, whereas seeders and shrubs had negative effects. The marginal R^2 was 0.18, and the conditional R^2 reached 0.57, indicating a moderate contribution of fixed predictors and a substantial influence of random effects.

At 24 months post-fire, the main effect of SPEI was no longer significant, although the interaction remained significant. During this period, all functional traits contributed positively to *T-LAI*. However, the explanatory power of the fixed effects decreased (marginal $R^2 = 0.13$), while the variance explained by the random effects increased (conditional $R^2 = 0.69$).

At 36 months, the interaction persisted, with a mean coefficient of 0.037, and the model's explanatory capacity improved notably (marginal $R^2 = 0.25$), primarily driven by the positive effect of all functional traits considered. From 48 months onwards, 100 % of the models indicated no significant effect of the climatic variables (neither the main effect of SPEI nor its interaction).

Overall, these results suggest that the influence of climate on *T-LAI* is strongest in the early years following fire. As the SPEI accumulation window expands, the direct effect of climate loses significance, while the interaction with burn condition and, especially, the contribution of the affected vegetation's functional traits become increasingly relevant.

4. Discussion

4.1. *T-LAI* as post-fire vegetation recovery indicator

We opted for a complex data product such as the MODIS LAI product to quantify post-fire vegetation recovery (Putzenlechner et al., 2024) and interpret it from a biophysical perspective. LAI is a useful parameter in forestry and serves as an indicator of forest productivity, due to its close association with essential processes such as photosynthesis,

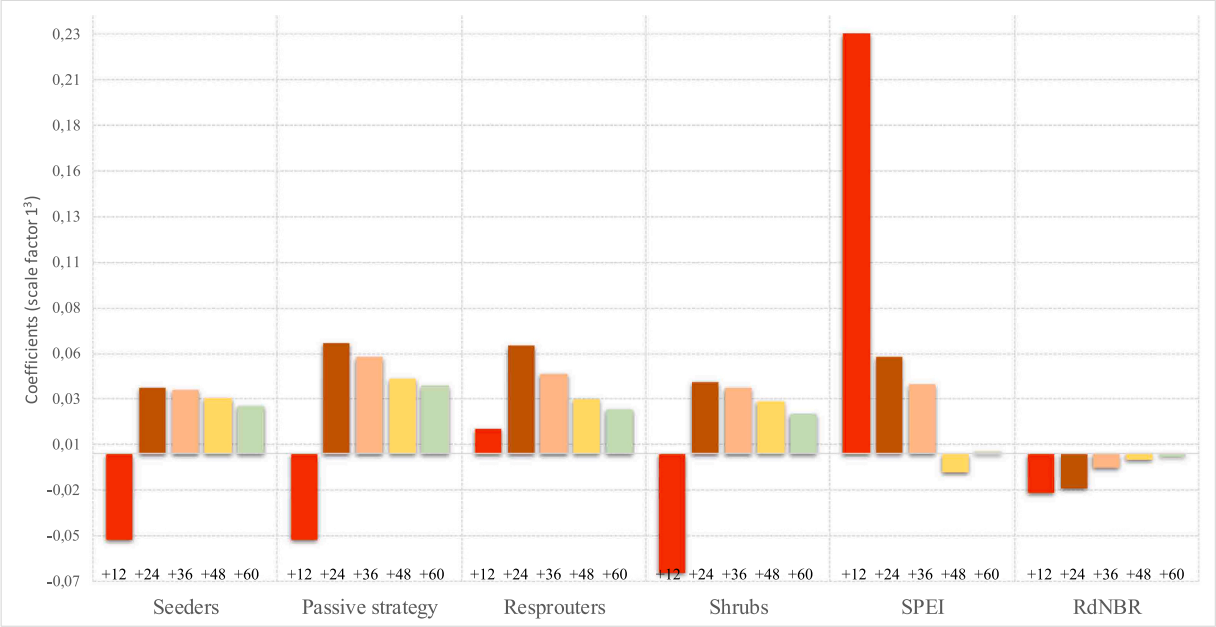

Fig. 5. Mean coefficients (scale factor 1^3) of fixed factors in the explanatory function of *T-LAI* over the post-fire periods (+12 to +60 months). Each block represents a specific explanatory factor: seeders, passive, resprouter, shrubs, SPEI, and RdNBR.

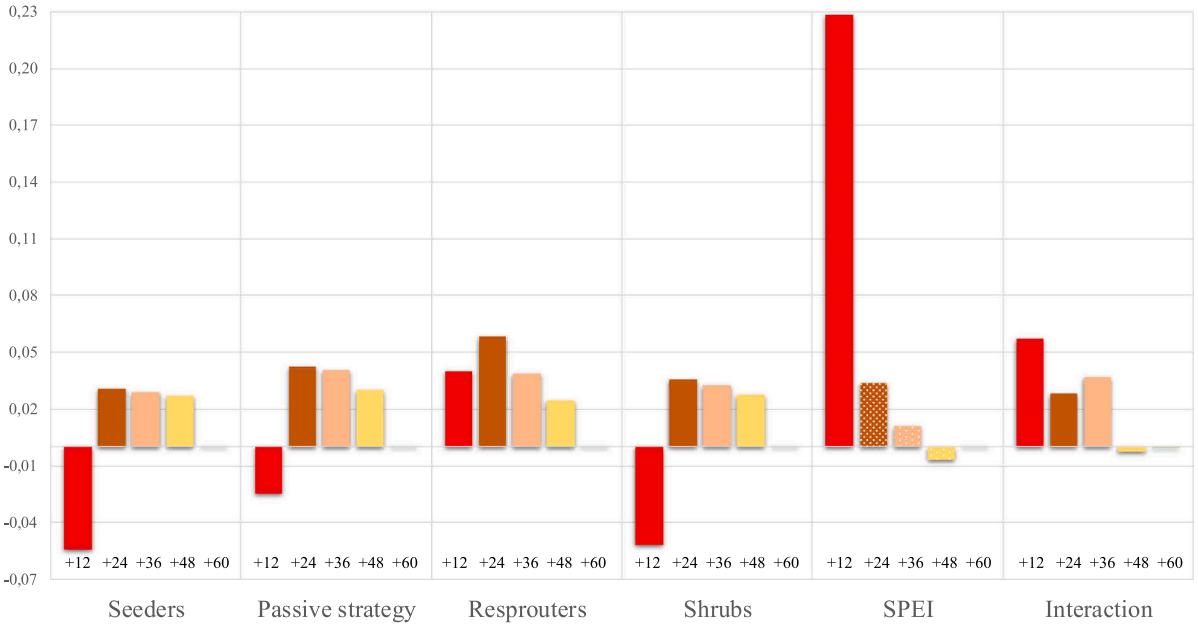

Fig. 6. Mean coefficients (scale factor 1^3) of fixed factors in the explanatory function of *T-LAI* over the post-fire periods (+12 to +60 months). Each block represents a specific explanatory factor: seeders, passive, resprouter, shrubs, SPEI, and Interaction.

transpiration-respiration, evapotranspiration, interception and gross primary productivity of vegetation (Alton, 2018; Asner et al., 2003; Boussetta et al., 2013; Jarlan et al., 2008). Its use is widespread in carbon circulation models, climate models, and ecological models (Keenan et al., 2009; Sabateé et al., 2002; Wang et al., 2019).

In the case of burned areas, spectral recovery cannot always be directly associated with the ecological recovery of the affected vegetation types (Celebrezze et al., 2024). However, *T-LAI* can be used as a proxy for the recovery of physiological functionality in terms of leaf area over time periods of varying lengths. Although resilience analysis requires numerous metrics for a comprehensive diagnosis (Hodgson et al., 2015; Falk et al., 2022), the use of *T-LAI* provides a more precise magnitude in relation to the recovery of vegetation structure and may bring us closer to the concept of recovery in eco-physiological terms (Folke et al., 2010). Furthermore, the cumulative time perspective, from 1 to 5 post-fire years, allows the interpretation of the trend relative to the estimation window and establishes a direct connection with the multi-scalar dimension of the SPEI.

In the first post-fire year, trend sign and magnitude showed high variability, often negative, reflecting the complexity of natural adjustments to new environmental conditions. Vegetation mortality (lightly scorched or partially affected) may coexist with rapid herbaceous growth and opportunistic species, alongside hydro-geomorphological processes that may inhibit regeneration. The regeneration lag

observed in the first + 12 months may also be partly influenced by the spectral response of persistent combustion products (Montorio et al., 2020) and partially burned vegetation, as well as by the potential impact of hydrological-forestry treatments, such as extraction and/or in situ management of burned wood(Vlassova and Pérez-Cabello, 2016), which could introduce additional uncertainty in surface reflectance patterns. For example, these post-fire treatments can alter the optical properties of the affected areas by decreasing reflectance in some spectral bands (e.g., shortwave infrared) while increasing it in others (e.g., near-infrared), thereby modifying the spectral signal associated with natural regeneration of the vegetation.

In addition, potential misclassification of land cover may also contribute to uncertainties in MODIS-derived LAI estimates, as the biome-specific lookup tables applied by the LAI/FPAR algorithm (MCD15A2H) may not reflect the actual structural changes in vegetation caused by fire, particularly in areas undergoing strong transitions (Pu et al., 2020; Lv et al., 2024).

The variability in the first period (+12 m) contrasted with the widespread, more intensive growth observed in the first + 24 months, followed by stabilization after + 36 months. This highlights the importance of selecting appropriate time gaps to capture different dimensions of ecosystem responses to both direct and indirect fire effects, particularly when using variables based on the spectral response of post-fire vegetation cover (Chu and Guo, 2013; Meng et al., 2018).

4.2. Modeling *T-LAI* values extracted from MODIS

Using multiscale *T-LAI* values to analyze factors driving its direction and magnitude, we evaluated the influence of burn severity, SPEI values, and pre-fire vegetation type on regenerative trends. In addition, for SPEI—the only exogenous factor affecting both burned and unburned areas—we assessed whether its influence on burned areas reflects a genuine post-fire recovery or merely replicates the general climatic response.

To capture variability and avoid underestimation, fire location was included as a random effect in the GLMM. This approach accounted for ecological complexity, where both constant factors and variable conditions, represented by random effects, influence vegetation recovery. The results were consistent with existing literature and emphasized the relevance of fixed factors depending on their proximity to the fire event, given the varying durations of the analysis periods.

4.2.1. Fixed factors

The SPEI provides a representative measure of water balance that is crucial for assessing its impact on vegetation recovery when analyzing the influence of post-fire moisture conditions on *T-LAI* values. Due to its multiscale analysis capabilities, the SPEI has been widely used in studies to quantify its effect on post-fire recovery (e.g., Viana-Soto et al., 2020).

In our case, considering that episodes of ecological drought (Crausbay et al., 2017), capable of exceeding biological tolerance thresholds and altering natural systems, occurred throughout the post-fire period, the results obtained indicated that wet conditions had a positive influence on the regenerative trend of *T-LAI*. This effect, based on the statistical significance and the magnitude and direction of the coefficients derived from the multiscale modeling, was particularly relevant during the first months after the fire. Moreover, based on the modeling that incorporates the SPEI–FIRE interaction, the results indicate that the influence of SPEI on *T-LAI* is more pronounced in burned areas than in unburned ones, especially during the first years following the fire. This conclusion is supported by the statistical significance of the interaction, which reveals a modulation of the climatic effect depending on whether the area was burned or served as control. In particular, at shorter temporal scales (12–36 months), this interaction is significant, suggesting that drought/wetness conditions play a critical role in the initial stages of postfire regeneration. This pattern supports the hypothesis that climate acts as a key limiting factor in the recovery trajectory of fire-affected vegetation, whereas its influence is more diffuse in unaffected ecosystems.

Our results align with previous studies that also analyzed the impact of climatic conditions on post-fire recovery using spectral variables. For example, Blanco-Rodríguez et al., (2023) highlighted the influence of climate on vegetation regeneration during the first years after fire, and the significant role of drought in reducing Mediterranean forest recovery. Similarly, Storey et al. (2021), using a 35-year series of Landsat images and a predictor related to climatic water deficit, also reported significant associations.

Our results are also consistent with the current scientific interest in analyzing the effects of climate change on both fire regime transformations and post-fire recovery processes. Regarding the latter and considering the role of moisture conditions in ensuring mid-term (3–5 years) post-fire foliar growth, predictions of increased drought frequency and intensity (Gomez-Gomez et al., 2022; Miller et al., 2009; Miller and Thode, 2007; Tramblay et al., 2020) could negatively impact future fire recovery processes. This is due to changes in the structure and composition of affected ecosystems (Bendall et al., 2022; Parks and Abatzoglou, 2020).

For the burn severity analysis using Landsat imagery, we used the RdNBR to mitigate the bias associated with pre-fire vegetation characteristics in the distribution of severity values. This adjustment helped to reduce the overestimation of severity in areas with higher pre-fire vegetation density while preventing the systematic association of low-cover areas with low severity. Such misclassification could have significant consequences for regenerative trends (i.e., misclassified areas, as low severity could be linked to high intercepts and low slopes in recovery models). Conversely, severely burned areas, which generally correspond to zones with higher pre-fire vegetation density, tended to exhibit steeper slopes in the models, which could be misinterpreted as faster LAI recovery.

The results obtained are consistent with Keeley (2009), who identified the negative influence of this contextual factor on vegetation recovery. This relationship between high severity levels and lower regeneration is still recognized in numerous recently published studies. For example, based on a systematic review, Grau-Andrés et al. (2024) provided global evidence that high severity negatively affects vegetation abundance, diversity, and overall condition. This was attributed to the impact of extreme temperatures on the insulating capacity of the bark and the destruction of the regenerative structures of the affected species. Volkova et al. (2025a) indicated that, although burn severity did not have a significant impact on species richness, diversity, or composition, it led to notable changes in the specific composition of affected ecosystems. This suggests that high-severity fires create environmental conditions that differ from those in unburned areas or regions affected by low-severity fires.

However, in our case, the influence of burn severity was only moderate and decreased as the time scale expanded (~50 % of the models lost the significance of this factor when the period was extended from +24 to +36 months (Table 5)). The explanatory power of the burn severity was particularly evident when considering the quantified trends

Table 5
Percentage of models with variables showing statistical significance. Distribution by accumulated post-fire time intervals.

	*T-LAI*_1st$_{+12}$	*T-LAI*_2nd$_{+24}$	*T-LAI*_3rd$_{+36}$	*T-LAI*_4th$_{+48}$	*T-LAI*_5th$_{+60}$
(Intercept)	100	100	100	100	100
Seeders	100	**100**	100	100	100
Passive strategy	85	**100**	100	100	100
Resprouters	8	**100**	100	100	100
Shrubs	100	**100**	100	100	100
SPEI	**100**	0	28	0	0
RdNBR	5	**92**	42	2	1

for the first + 24 months. Similarly, Caccamo et al. (2015), using MODIS data, also concluded that the influence of severity was limited to the first + 24 months.

Regeneration mechanism played a significant role in all models (*p-value* < 0.05 in 100 % of cases), and although its influence decreased slightly as the analysis period increased, it never lost statistical significance. This effect was particularly important in resprouting tree species or those with a passive recovery strategy. In this context, the successional process following fire–considered as a disturbance in the sense of Sousa (1984)–can be described as a process of reestablishment of the affected systems (Herranz Sanz, 2000). However, in this study, only the autosuccession of foliar fraction levels can be addressed, as other aspects, such as physiognomic recovery or the reestablishment of pre-fire species composition, remain opaque Table 6.

4.2.2. *Changes in influence depending on post-fire cumulative time periods*

According to previous studies, both burn severity and post-fire climatic conditions significantly influence the regenerative dynamics of affected ecosystems (Meng et al., 2015; Volkova et al., 2025b). However, the magnitude of this contribution varied depending on the temporal scale analyzed. In general terms, the regenerative trend during the first + 12 months showed negative average values. This may be related to the temporal proximity of the fire event and the lack of time for the ecosystem to start recovering from the impact. In the early stages, affected ecosystems exhibited marked instability due to the adaptation process to new environmental conditions and the direct effects of fire. During this period, regenerative processes coexisted with potential hydro-geomorphological reactivation (e.g., soil loss and/or fertility decline), which can significantly inhibit natural regeneration.

Notably, there was a significant negative effect of regeneration mechanisms, attributed to the influence of vegetation on the intercepts of functions related to LAI trends. In fact, similar studies have excluded this period from recovery analyses (Meng et al., 2015), as vegetation in the first post-fire year may continue to lose vigor due to the radiometric impact of combustion residues or to reduced photosynthetic activity resulting from post-fire management actions, such as hydrological control measures and burned wood removal (Solans Vila and Barbosa, 2010).

On the other hand, positive regeneration was primarily associated with wet climatic conditions (positive SPEI anomalies), while burn severity had a negative influence, although it was less relevant than post-fire climatic conditions.

During the first two years, a significant change was observed in the influence of fixed factors related to vegetation. Positive climatic anomalies continued to exert a positive effect on the regeneration process, although this effect was not statistically significant (p-value > 0.05) and had a much smaller impact compared to the trend observed in the first 12 months. On the other hand, burn severity maintained the same intensity in the models, but with greater statistical significance: over 90 % of the models showed a statistically significant effect. However, the most notable changes were observed in the influence of the occupation percentages of species according to their dominant regeneration mechanism. In contrast to the role they played in the + 12-month model, these factors were positive and significant in all cases.

Table 6
Percentage of models with variables showing statistical significance. Distribution by accumulated post-fire time intervals.

	$t\text{-}lai\_1^{st}_{+12}$	$t\text{-}lai\_2^{nd}_{+24}$	$t\text{-}lai\_3^{rd}_{+36}$	$t\text{-}lai\_4^{th}_{+48}$	$t\text{-}lai\_5^{th}_{+60}$
(Intercept)	100	100	100	100	100
Seeders	100	**100**	100	100	100
Passive strategy	51,8	**100**	100	100	100
Resprouters	95,1	**100**	100	100	100
Shrubs	100	**100**	100	100	100
SPEI	**100**	0	0	0	0
Interaction	82,4	**96,6**	100	0,2	0,7

This effect was particularly notable in resprouting tree species and in systems dominated by passive regeneration mechanisms (e.g., Scots pine and black pine forests), which had greater weight in the model.

In periods longer than + 24 months, the ecosystems showed clear signs of stabilization and regeneration. This process was driven by the preexisting species in tree vegetation types dominated by seeding and resprouting species, as well as the regeneration of latent shrublands present in the understory of pine forests with a passive strategy. These results were consistent with those described in previous studies on the regenerative trajectories of these vegetation types in the regional analysis of Aragón.

During the three-year post-fire period, the role of regeneration mechanisms remained significant, although with a slightly reduced influence compared to the previous periods. Burn severity showed a slight decrease in its impact, as well as in the percentage of models where its effect was statistically significant (around 40 %). Similarly, the specific weight of climatic factors also decreased and was significant in only 28 % of the models.

As longer periods were included in the analysis of LAI trends, changes in the slope tended to stabilize, approaching values near zero and reducing the variability observed in shorter periods. After 36 months, the trends reached neutral or very mild levels, stabilizing around zero. In contrast, at the onset of regeneration, a more pronounced negative character and greater dispersion of trends were observed.

5. Conclusion

This study analyzes the influence of post-fire climatic conditions through the SPEI, burn severity, and characteristics of the affected vegetation using the LAI regenerative trend. The analysis considers post-fire periods of varying durations and takes into account forest fires that occurred between 2003 and 2015, distributed across contrasting biogeographical environments in Aragón (northeastern Spain).

Using the LAI trend as a regeneration indicator allowed assessment of vegetation recovery through changes in leaf fraction and its regulatory processes, including canopy interception, evapotranspiration, and net primary productivity. During the first months after the fire, LAI trends were highly variable, often showing negative trends. However, when considering a longer period of up to + 24 months, more pronounced and predominantly positive trends were observed. Beyond + 36 months, these trends decreased in intensity and tended to stabilize as the analysis period lengthened (more than +36 months post-fire). Likewise, the influence of SPEI on the LAI trend is more evident in fire-affected areas than in control zones, although only during the first years following the fire.

Burn severity and particularly the moisture conditions in the year following the fire, directly influenced the regenerative dynamics of the leaf fraction in the affected ecosystems. In this context, reduced soil moisture due to climatic anomalies could inhibit or delay the effectiveness of regeneration mechanisms or lead to higher mortality scenarios as a consequence of the fire.

Furthermore, the regeneration mechanism of the species emerged as a significant factor in the regenerative trend of the LAI, although its relevance progressively decreased as the analysis period lengthened. This effect was particularly pronounced in tree species with sprouting capacity or passive regeneration strategies.

Future climate aridification scenarios could further slow down regeneration rates, even in Mediterranean ecosystems with effective regeneration mechanisms. These findings may help to calibrate simulation models of post-fire dynamics, enhancing management strategies to safeguard ecosystem services.

CRediT authorship contribution statement

Raquel Montorio: Writing – review & editing, Supervision,

Software, Investigation. **Cristian Iranzo:** Supervision, Software, Resources, Investigation, Conceptualization. **Roberto Serrano-Notivoli:** Writing – review & editing, Writing – original draft, Resources, Methodology, Conceptualization. **Fernando Pérez-Cabello:** Writing – review & editing, Writing – original draft, Methodology, Investigation, Formal analysis, Conceptualization.

Funding

This research was supported by the project Dynamic Analysis of the Resilience of Fire-Affected Forest Landscapes Using Multisensor Spectral Indicators (Grant PID2020–118886RB-I00), funded by MCIN/AEI/10.13039/501100011033.

R.S.-N. is funded by the grant RYC2021–034330-I from MCIN/AEI/10.13039/501100011033 and by the European Union NextGenerationEU/PRTR. Additionally, he receives support from the Government of Aragón through the Programme of Research Groups (Group S74_23R, Clima, Agua, Cambio Global y Sistemas Naturales).

C.I.-C. is funded by the Government of Aragón through a doctoral grant (2022–2026 call).

Declaration of Competing Interest

The authors declare that they have no known competing financial interests or personal relationships that could have appeared to influence the work reported in this paper.

Appendix A. Supporting information

Supplementary data associated with this article can be found in the online version at doi:10.1016/j.foreco.2026.123568.

Data availability

Data will be made available on request.

References

Alcañiz, M., Outeiro, L., Francos, M., Úbeda, X., 2018. Effects of prescribed fires on soil properties: a review. Sci. Total Environ. 613–614, 944–957. https://doi.org/10.1016/j.scitotenv.2017.09.144.

Alton, P.B., 2018. Decadal trends in photosynthetic capacity and leaf area index inferred from satellite remote sensing for global vegetation types. Agric. For. Meteor. 250–251, 361–375. https://doi.org/10.1016/j.agrformet.2017.11.020.

Alvarez, R., Valbuena, L., Calvo, L., 2005. Influence of tree age on seed germination response to environmental factors and inhibitory substances in Pinus pinaster. Int. J. Wildl. Fire 14, 277–284. https://doi.org/10.1071/WF04066.

Arizpe, A.H., Falk, D.A., Woodhouse, C.A., Swetnam, T.W., 2020. Widespread fire years in the US–Mexico Sky Islands are contingent on both winter and monsoon precipitation. Int. J. Wildland Fire 29, 1072–1087. https://doi.org/10.1071/WF19181.

Asner, G.P., Scurlock, J.M.O., A. Hicke, J., 2003. Global synthesis of leaf area index observations: implications for ecological and remote sensing studies. Glob. Ecol. Biogeogr. 12, 191–205. https://doi.org/10.1046/j.1466-822X.2003.00026.x.

Baeza, M.J., Vallejo, V.R., 2008. Vegetation Recovery after Fuel Management in Mediterranean Shrublands. Appl. Veg. Sci. 11, 151–158.

Bendall, E.R., Bedward, M., Boer, M., Clarke, H., Collins, L., Leigh, A., Bradstock, R.A., 2022. Mortality and resprouting responses in forest trees driven more by tree and ecosystem characteristics than drought severity and fire frequency. For. Ecol. Manag. 509, 120070. https://doi.org/10.1016/j.foreco.2022.120070.

Blanco-Rodríguez, M.Á., Ameztegui, A., Gelabert, P., Rodrigues, M., Coll, L., 2023. Short-term recovery of post-fire vegetation is primarily limited by drought in Mediterranean forest ecosystems. Fire Ecol. 19, 68. https://doi.org/10.1186/s42408-023-00228-w.

Bolker, B.M., Brooks, M.E., Clark, C.J., Geange, S.W., Poulsen, J.R., Stevens, M.H.H., White, J.S.S., 2009. Generalized linear mixed models: a practical guide for ecology and evolution. Trends Ecol. Evol. 24, 127–135. https://doi.org/10.1016/j.tree.2008.10.008.

Bond, W.J., Keeley, J.E., 2005. Fire as a global "herbivore": The ecology and evolution of flammable ecosystems. Trends Ecol. Evol. 20, 387–394. https://doi.org/10.1016/j.tree.2005.04.025.

Bond, W.J., Woodward, F.I., Midgley, G.F., 2005. The Global Distribtuion of Ecosystems in a world without Fire. N. Phytol. 165, 525–538. https://doi.org/10.1111/j.1469-8137.2004.01252.x.

Borini Alves, D., Pérez-Cabello, F., Rodrigues Mimbrero, M. Land-use and land-cover dynamics monitored by NDVI multitemporal analysis in a selected southern amazonian area (Brazil) for the last three decades, in: International Archives of the Photogrammetry, Remote Sensing and Spatial Information Sciences - ISPRS Archives. pp. 329–335. https://doi.org/10.5194/isprsarchives-XL-7-W3-329-2015.

Boussetta, S., Balsamo, G., Beljaars, A., Kral, T., Jarlan, L., 2013. Impact of a satellite-derived leaf area index monthly climatology in a global numerical weather prediction model. Int. J. Remote Sens 34, 3520–3542. https://doi.org/10.1080/01431161.2012.716543.

Bright, B.C., Hudak, A.T., Kennedy, R.E., Braaten, J.D., Henareh Khalyani, A., 2019. Examining post-fire vegetation recovery with Landsat time series analysis in three western North American forest types. Fire Ecol. 15, 8. https://doi.org/10.1186/s42408-018-0021-9.

Caccamo, G., Bradstock, R., Collins, L., Penman, T., Watson, P., 2015. Using MODIS data to analyse post-fire vegetation recovery in Australian eucalypt forests. J. Spat. Sci. 60, 341–352. https://doi.org/10.1080/14498596.2015.974227.

Carlson, T.N., Perry, E.M., Schmugge, T.J., 1990. Remote estimation of soil moisture availability and fractional vegetation cover for agricultural fields. Agric. For. Meteor. 52, 45–69. https://doi.org/10.1016/0168-1923(90)90100-K.

Caturla, R.N., Raventós, J., Guàrdia, R., Vallejo, V.R., 2000. Early post-fire regeneration dynamics of Brachypodium retusum Pers. (Beauv.) in old fields of the Valencia region (eastern Spain). Acta Oecologica 21, 1–12. https://doi.org/10.1016/S1146-609X(00)00114-4.

Celebrezze, J.V., Franz, M.C., Andrus, R.A., Stahl, A.T., Steen-Adams, M., Meddens, A.J. H., 2024. A fast spectral recovery does not necessarily indicate post-fire forest recovery. Fire Ecol. 20. https://doi.org/10.1186/s42408-024-00288-6.

Chen, J.M., Black, T.A., 1992. Defining leaf area index for non-flat leaves. Plant. Cell Environ. 15, 421–429. https://doi.org/10.1111/j.1365-3040.1992.tb00992.x.

Chu, T., Guo, X., 2013. Remote Sensing Techniques in Monitoring Post-Fire Effects and Patterns of Forest Recovery in Boreal Forest Regions: A Review. Remote Sens 6, 470–520. https://doi.org/10.3390/rs6010470.

Clarke, P.J., Lawes, M.J., Midgley, J.J., Lamont, B.B., Ojeda, F., Burrows, G.E., Enright, N.J., Knox, K.J.E., 2013. Resprouting as a key functional trait: how buds, protection and resprouting ability shape plant responses to disturbance. N. Phytol. 197, 19–35. https://doi.org/10.1111/nph.12001.

Cleveland, R.B., Cleveland, W.S., McRae, J.E., Terpenning, I., 1990. STL: A seasonal-trend decomposition. J. Off. Stat. 6, 3–73.

Cocke, A.E., Fulé, P.Z., Crouse, J.E., 2005. Comparison of burn severity assessments using Differenced Normalized Burn Ratio and ground data. Int. J. Wildl. Fire 14, 189. https://doi.org/10.1071/WF04010.

Crausbay, S.D., Ramirez, A.R., Carter, S.L., Cross, M.S., Hall, K.R., Bathke, D.J., Betancourt, J.L., Colt, S., Cravens, A.E., Dalton, M.S., Dunham, J.B., Hay, L.E., Hayes, M.J., McEvoy, J., McNutt, C.A., Moritz, M.A., Nislow, K.H., Raheem, N., Sanford, T., 2017. Defining Ecological Drought for the Twenty-First Century. Bull. Am. Meteorol. Soc. 98, 2543–2550. https://doi.org/10.1175/BAMS-D-16-0292.1.

Crockett, J.L., Hurteau, M.D., 2024. Ability of seedlings to survive heat and drought portends future demographic challenges for five southwestern US conifers. Tree Physiol. 44, 1–13. https://doi.org/10.1093/treephys/tpad136.

Daskalakou, E.N., Thanos, C.A., 2004. Postfire regeneration of Aleppo pine - The temporal pattern of seedling recruitment. Plant Ecol. 171, 81–89. https://doi.org/10.1023/B:VEGE.0000029375.93419.f9.

Desrochers, M.L., Clippard, E.A., Johnson, L.K., Beier, C.M., 2025. Declining trends in canopy disturbance across reserve forest landscapes of the northeastern US. For. Ecol. Manag. 578, 122463. https://doi.org/10.1016/j.foreco.2024.122463.

Doblas-Miranda, E., Alonso, R., Arnan, X., Bermejo, V., Brotons, L., de las Heras, J., Estiarte, M., Hódar, J.A., Llorens, P., Lloret, F., López-Serrano, F.R., Martínez-Vilalta, J., Moya, D., Peñuelas, J., Pino, J., Rodrigo, A., Roura-Pascual, N., Valladares, F., Vilà, M., Zamora, R., Retana, J., 2017. A review of the combination among global change factors in forests, shrublands and pastures of the Mediterranean Region: Beyond drought effects. Glob. Planet. Change 148, 42–54. https://doi.org/10.1016/j.gloplacha.2016.11.012.

Donato, D.C., Fontaine, J.B., Campbell, J.L., Robinson, W.D., Kauffman, J.B., Law, B.E., 2009. Conifer regeneration in stand-replacement portions of a large mixed-severity wildfire in the klamath-siskiyou mountains. Can. J. For. Res. 39, 823–838. https://doi.org/10.1139/X09-016.

Epting, J., Verbyla, D., Sorbel, B., 2005. Evaluation of remotely sensed indices for assessing burn severity in interior Alaska using Landsat TM and ETM+. Remote Sens. Environ. 96, 328–339. https://doi.org/10.1016/j.rse.2005.03.002.

Falk, D.A., van Mantgem, P.J., Keeley, J.E., Gregg, R.M., Guiterman, C.H., Tepley, A.J., JN Young, D., Marshall, L.A., 2022. Mechanisms of forest resilience. For. Ecol. Manag. 512, 120129. https://doi.org/10.1016/j.foreco.2022.120129.

Fang, H., Baret, F., Plummer, S., Schaepman-Strub, G., 2019. An Overview of Global Leaf Area Index (LAI): Methods, Products, Validation, and Applications. Rev. Geophys 57, 739–799. https://doi.org/10.1029/2018RG000608.

Fernández-García, V., Fulé, P.Z., Marcos, E., Calvo, L., 2019. The role of fire frequency and severity on the regeneration of Mediterranean serotinous pines under different environmental conditions. For. Ecol. Manag. 444, 59–68. https://doi.org/10.1016/j.foreco.2019.04.040.

Folke, C., Carpenter, S.R., Walker, B., Scheffer, M., Chapin, T., Rockström, J., 2010. Resilience thinking: Integrating resilience, adaptability and transformability. Ecol. Soc. 15. https://doi.org/10.5751/ES-03610-150420.

French, N.H.F., Kasischke, E.S., Hall, R.J., Murphy, K.A., Verbyla, D.L., Hoy, E.E., Allen, J.L., 2008. Using Landsat data to assess fire and burn severity in the North American boreal forest region: An overview and summary of results. Int. J. Wildl. Fire 17, 443–462. https://doi.org/10.1071/WF08007.

Ganguly, S., Nemani, R.R., Zhang, G., Hashimoto, H., Milesi, C., Michaelis, A., Wang, W., Votava, P., Samanta, A., Melton, F., Dungan, J.L., Vermote, E., Gao, F., Knyazikhin, Y., Myneni, R.B., 2012. Generating global Leaf Area Index from Landsat: Algorithm formulation and demonstration. Remote Sens. Environ. 122, 185–202. https://doi.org/10.1016/j.rse.2011.10.032.

Garcia-Villanueva, J., Ena, V., Tarrega, R., Mediavilla, G., 1998. Recolonization of Two Burnt Quercus pyrenaica Ecosystems by Coleoptera. Int. J. Wildl. Fire 8, 21–27. https://doi.org/10.1071/WF9980021.

Garrigues, S., Lacaze, R., Baret, F., Morisette, J.T., Weiss, M., Nickeson, J.E., Fernandes, R., Plummer, S., Shabanov, N.V., Myneni, R.B., Knyazikhin, Y., Yang, W., 2008. Validation and intercomparison of global Leaf Area Index products derived from remote sensing data. J. Geophys. Res. Biogeosci 113, G02028. https://doi.org/10.1029/2007JG000635.

Gitas, I., Mitri, G., Veraverbeke, S., Polychronaki, A., 2012. Advances in Remote Sensing of Post-Fire Vegetation Recovery Monitoring - A Review. Remote Sens. Biomass.. Princ. Appl. https://doi.org/10.5772/20571.

Gomez-Gomez, J.-D., Pulido-Velazquez, D., Collados-Lara, A.-J., Fernandez-Chacon, F., 2022. The impact of climate change scenarios on droughts and their propagation in an arid Mediterranean basin. A useful approach for planning adaptation strategies. Sci. Total Environ. 820, 153128. https://doi.org/10.1016/j.scitotenv.2022.153128.

Grau-Andrés, R., Moreira, B., Pausas, J.G., 2024. Global plant responses to intensified fire regimes. Glob. Ecol. Biogeogr. 33. https://doi.org/10.1111/geb.13858.

Harvey, B.J., Donato, D.C., Turner, M.G., 2016. High and dry: post-fire tree seedling establishment in subalpine forests decreases with post-fire drought and large stand-replacing burn patches. Glob. Ecol. Biogeogr. 25, 655–669. https://doi.org/10.1111/geb.12443.

Herranz Sanz, J.M., 2000. Aspectos botánicos y ecológicos del Pino carrasco (Pinus halepensis Mill.). Cuad. De. la Soc. Española De. Cienc. For. 17, 13–17.

Hodgson, D., McDonald, J.L., Hosken, D.J., 2015. What do you mean, "resilient"? Trends Ecol. Evol. 30, 503–506. https://doi.org/10.1016/j.tree.2015.06.010.

Jarlan, L., Balsamo, G., Lafont, S., Beljaars, A., Calvet, J.C., Mougin, E., 2008. Analysis of leaf area index in the ECMWF land surface model and impact on latent heat and carbon fluxes: Application to West Africa. J. Geophys. Res. Atmos. 113. https://doi.org/10.1029/2007JD009370.

Jiménez Ruano, A., Pérez-Cabello, F., Montorio Llovería, R., 2016. Niveles de LAI/fPAR en superficies afectadas por incendios forestales en Aragón. Análisis mediante el producto MCD15A2 de MODIS. Pirineos 171, 1–13. https://doi.org/10.3989/Pirineos.2016.171003.

Justice, C.O., Giglio, L., Korontzi, S., Owens, J., Morisette, J.T., Roy, D., Descloitres, J., Alleaume, S., Petitcolin, F., Kaufman, Y., 2002. The MODIS fire products. Remote Sens. Environ. 83, 244–262. https://doi.org/10.1016/S0034-4257(02)00076-7.

Kapsomenakis, J., Douvis, C., Poupkou, A., Zerefos, S., Solomos, S., Stavraka, T., Melis, N.S., Kyriakidis, E., Kremlis, G., Zerefos, C., 2023. Climate change threats to cultural and natural heritage UNESCO sites in the Mediterranean. Environ. Dev. Sustain 25, 14519–14544. https://doi.org/10.1007/s10668-022-02677-w.

Karavani, A., Boer, M.M., Baudena, M., Colinas, C., Díaz-Sierra, R., Pemán, J., de Luis, M., Enríquez-de-Salamanca, Á., Resco de Dios, V., 2018. Fire-induced deforestation in drought-prone Mediterranean forests: drivers and unknowns from leaves to communities. Ecol. Monogr. 88, 141–169. https://doi.org/10.1002/ecm.1285.

Kazanis, D., Arianoutsou, M., 1996. Vegetation Composition in a Post-Fire Successional Gradient of Pinus halepensis Forests in Attica, Greece. Int. J. Wildl. Fire 6, 83–91. https://doi.org/10.1071/WF9960083.

Keeley, J.E., 2009. Fire intensity, fire severity and burn severity: a brief review and suggested usage. Int. J. Wildl. Fire 18, 116. https://doi.org/10.1071/WF07049.

Keeley, J.E., Pausas, J.G., Rundel, P.W., Bond, W.J., Bradstock, R.A., 2011. Fire as an evolutionary pressure shaping plant traits. Trends Plant Sci. 16, 406–411. https://doi.org/10.1016/j.tplants.2011.04.002.

Keenan, T., García, R., Friend, A.D., Zaehle, S., Gracia, C., Sabate, S., 2009. Improved understanding of drought controls on seasonal variation in Mediterranean forest canopy CO 2 and water fluxes through combined in situ measurements and ecosystem modelling. Biogeosciences 6, 1423–1444. https://doi.org/10.5194/bg-6-1423-2009.

Kendall, M.G., 1975. Rank Correlation Methods, 4th editio. ed. Charles Griffin, London.

Key, C.H., Benson, N.C., 2006. Landscape assessment: Sampling and analysis methods. USDA For. Serv. Gen. Tech. Rep. RMRS-GTR-164-CD 1–55.

Knyazikhin, Y., Martonchik, J.V., Myneni, R.B., Diner, D.J., Running, S.W., 1998. Synergistic algorithm for estimating vegetation canopy leaf area index and fraction of absorbed photosynthetically active radiation from MODIS and MISR data. J. Geophys. Res. Atmos. 103, 32257–32275. https://doi.org/10.1029/98JD02462.

Lalor, A.R., Law, D.J., Breshears, D.D., Falk, D.A., Field, J.P., Loehman, R.A., Triepke, F. J., Barron-Gafford, G.A., 2023. Mortality thresholds of juvenile trees to drought and heatwaves: implications for forest regeneration across a landscape gradient. Front. For. Glob. Chang 6, 1–16. https://doi.org/10.3389/ffgc.2023.1198156.

Lentile, L.B., Holden, Z. a, Smith, A.M.S., Falkowski, M.J., Hudak, A.T., 2006. Remote sensing techniques to assess active fire characteristics and post fire effects. USDA For. Serv. / UNL Fac. Publ. 194, 319–345.

Lin, W., Yuan, H., Dong, W., Zhang, S., Liu, S., Wei, N., Lu, X., Wei, Z., Hu, Y., Dai, Y., 2023. Reprocessed MODIS Version 6.1 Leaf Area Index Dataset and Its Evaluation for Land Surface and Climate Modeling. Remote Sens 15, 1780. https://doi.org/10.3390/rs15071780.

Ling, X.L., Fu, C.B., Guo, W.D., Yang, Z.L., 2019. Assimilation of Remotely Sensed LAI Into CLM4CN Using DART. J. Adv. Model. Earth Syst. 11, 2768–2786. https://doi.org/10.1029/2019MS001634.

Lloret, F., 2004. Rígimen de incendios y regeneración. Ecol. Del. Bosque Mediterr. áneo En. Un. Mundo cambiante 101–126.

Lv, F., Sun, K., Li, W., Miao, S., Hu, X., 2024. Estimation of Leaf Area Index across Biomes and Growth Stages Combining Multiple Vegetation Indices. Sensors 24, 6106. https://doi.org/10.3390/s24186106.

Marcos, B., Gonçalves, J., Alcaraz-Segura, D., Cunha, M., Honrado, J.P., 2023. Assessing the resilience of ecosystem functioning to wildfires using satellite-derived metrics of post-fire trajectories. Remote Sens. Environ. 286. https://doi.org/10.1016/j.rse.2022.113441.

McClure, E.J., Coop, J.D., Guiterman, C.H., Margolis, E.Q., Parks, S.A., 2024. Contemporary fires are less frequent but more severe in dry conifer forests of the southwestern United States. Commun. Earth Environ. 5, 1–11. https://doi.org/10.1038/s43247-024-01686-z.

Meneses, B.M., 2021. Vegetation Recovery Patterns in Burned Areas Assessed with Landsat 8 OLI Imagery and Environmental Biophysical Data. Fire 4, 76. https://doi.org/10.3390/fire4040076.

Meng, R., Dennison, P.E., Huang, C., Moritz, M.A., D'Antonio, C., 2015. Effects of fire severity and post-fire climate on short-term vegetation recovery of mixed-conifer and red fir forests in the Sierra Nevada Mountains of California. Remote Sens. Environ. 171, 311–325. https://doi.org/10.1016/j.rse.2015.10.024.

Meng, R., Wu, J., Zhao, F., Cook, B.D., Hanavan, R.P., Serbin, S.P., 2018. Measuring short-term post-fire forest recovery across a burn severity gradient in a mixed pine-oak forest using multi-sensor remote sensing techniques. Remote Sens. Environ. 210, 282–296. https://doi.org/10.1016/j.rse.2018.03.019.

Miller, J.D., Safford, H.D., Crimmins, M., Thode, A.E., 2009. Quantitative evidence for increasing forest fire severity in the Sierra Nevada and southern Cascade Mountains, California and Nevada, USA. Ecosystems 12, 16–32. https://doi.org/10.1007/s10021-008-9201-9.

Miller, J.D., Thode, A.E., 2007. Quantifying burn severity in a heterogeneous landscape with a relative version of the delta Normalized Burn Ratio (dNBR). Remote Sens. Environ. 109, 66–80. https://doi.org/10.1016/j.rse.2006.12.006.

Montorio, R., Pérez-Cabello, F., Borini, D., García-martín, A., Borini Alves, D., García-martín, A., 2020. Unitemporal approach to fire severity mapping using multispectral synthetic databases and Random Forests. Remote Sens. Environ. 249, 112025. https://doi.org/10.1016/j.rse.2020.112025.

Moody, J.A., Shakesby, R.A., Robichaud, P.R., Cannon, S.H., Martin, D.A., 2013. Current research issues related to post-wildfire runoff and erosion processes. EarthSci. Rev. 122, 10–37. https://doi.org/10.1016/j.earscirev.2013.03.004.

Morisette, J.T., Baret, F., Privette, J.L., Myneni, R.B., Nickeson, J.E., Garrigues, S., Shabanov, N.V., Weiss, M., Fernandes, R.A., Leblanc, S.G., Kalacska, M., Sanchez-Azofeifa, G.A., Chubey, M., Rivard, B., Stenberg, P., Rautiainen, M., Voipio, P., Manninen, T., Pilant, A.N., Lewis, T.E., Iiames, J.S., Colombo, R., Meroni, M., Busetto, L., Cohen, W.B., Turner, D.P., Warner, E.D., Petersen, G.W., Seufert, G., Cook, R., 2006. Validation of global moderate-resolution LAI products: a framework proposed within the CEOS land product validation subgroup. IEEE Trans. Geosci. Remote Sens 44, 1804–1817. https://doi.org/10.1109/TGRS.2006.872529.

Moya, D., González-De Vega, S., García-Orenes, F., Morugán-Coronado, A., Arcenegui, V., Mataix-Solera, J., Lucas-Borja, M.E., De las Heras, J., 2018. Temporal characterisation of soil-plant natural recovery related to fire severity in burned Pinus halepensis Mill. forests. Sci. Total Environ. 640–641, 42–51. https://doi.org/10.1016/j.scitotenv.2018.05.212.

Neary, D.G., Ryan, K.C., DeBano, L.F., 2005. Wildland fire in ecosystems: effects of fire on soils and water. https://doi.org/10.2737/RMRS-GTR-42-V4.

Parks, S.A., Abatzoglou, J.T., 2020. Warmer and Drier Fire Seasons Contribute to Increases in Area Burned at High Severity in Western US Forests From 1985 to 2017. Geophys. Res. Lett. 47, 1–10. https://doi.org/10.1029/2020GL089858.

Parks, S.A., Holsinger, L.M., Koontz, M.J., Collins, L., Whitman, E., Parisien, M.A., Loehman, R.A., Barnes, J.L., Bourdon, J.F., Boucher, J., Boucher, Y., Caprio, A.C., Collingwood, A., Hall, R.J., Park, J., Saperstein, L.B., Smetanka, C., Smith, R.J., Soverel, N., 2019. Giving ecological meaning to satellite-derived fire severity metrics across North American forests. Remote Sens 11, 1–19. https://doi.org/10.3390/rs11141735.

Pausas, J.G., Bond, W.J., 2020. On the Three Major Recycling Pathways in Terrestrial Ecosystems. Trends Ecol. Evol. 35, 767–775. https://doi.org/10.1016/j.tree.2020.04.004.

Pausas, J.G., Bradstock, R.A., Keith, D.A., Keeley, J.E., Hoffman, W., Kenny, B., Lloret, F., Trabaud, L., 2004. Plant functional traits in relation to fire in crown-fire ecosystems. Ecology 85, 1085–1100. https://doi.org/10.1890/02-4094.

Pausas, J.G., Fernández-Muñoz, S., 2012. Fire regime changes in the Western Mediterranean Basin: From fuel-limited to drought-driven fire regime. Clim. Change 110, 215–226. https://doi.org/10.1007/s10584-011-0060-6.

Pausas, J.G., Keeley, J.E., 2009. A burning story: The role of fire in the history of life. Bioscience 59, 593–601. https://doi.org/10.1525/bio.2009.59.7.10.

Pausas, J.G., Keeley, J.E., 2014. Evolutionary ecology of resprouting and seeding in fire-prone ecosystems. N. Phytol. 204, 55–65. https://doi.org/10.1111/nph.12921.

Pausas, J.G., Vallejo, V.R., 1999. The role of fire in European Mediterranean Ecosystems. Remote Sens. Large Wildfires Eur. Mediterr. Basin 3–16.

Pu, J., Yan, K., Zhou, G., Lei, Y., Zhu, Y., Guo, D., Li, H., Xu, L., Knyazikhin, Y., Myneni, R.B., 2020. Evaluation of the MODIS LAI/FPAR Algorithm Based on 3D-RTM Simulations: A Case Study of Grassland. Remote Sens 12, 3391. https://doi.org/10.3390/rs12203391.

Putzenlechner, B., Bevern, F., Koal, P., Grieger, S., Koukal, T., Löw, M., Filipponi, F., Putzenlechner, B., Bevern, F., Koal, P., Grieger, S., 2024. Accuracy assessment of LAI, PAI and FCOVER from Sentinel-2 and GEDI for monitoring forests and their disturbance in Central Germany. Eur. J. Remote Sens 00. https://doi.org/10.1080/22797254.2024.2422323.

Pyne, S.J., 2007. Problems, paradoxes, paradigms: triangulating fire research. Int. J. Wildl. Fire 16, 271–276. https://doi.org/10.1071/WF06041.

Rajib, A., Kim, I.L., Golden, H.E., Lane, C.R., Kumar, S.V., Yu, Z., Jeyalakshmi, S., 2020. Watershed modeling with remotely sensed big data: Modis leaf area index improves hydrology and water quality predictions. Remote Sens 12, 1–17. https://doi.org/10.3390/rs12132148.

Rivas-Martínez, S., Rivas-Saenz, S., Penas, A., 2002. Worldwide Bioclimatic Classification System. Backhuys Pub, Kerkwerve, The Netherlands.

Rundel, P.W., Arroyo, M.T.K., Cowling, R.M., Keeley, J.E., Lamont, B.B., Vargas, P., 2016. Mediterranean Biomes: Evolution of Their Vegetation, Floras, and Climate. Annu. Rev. Ecol. Evol. Syst. 47, 383–407. https://doi.org/10.1146/annurev-ecolsys-121415-032330.

Russo, A., Gouveia, C.M., Páscoa, P., DaCamara, C.C., Sousa, P.M., Trigo, R.M., 2017. Assessing the role of drought events on wildfires in the Iberian Peninsula. Agric. For. Meteor. 237–238, 50–59. https://doi.org/10.1016/j.agrformet.2017.01.021.

Sabaté, S., Gracia, C.A., Sánchez, A., 2002. Likely effects of climate change on growth of Quercus ilex, Pinus halepensis, Pinus pinaster, Pinus sylvestris and Fagus sylvatica forests in the Mediterranean region. For. Ecol. Manag. 162, 23–37. https://doi.org/10.1016/S0378-1127(02)00048-8.

Saberi, S.J., Agne, M.C., Harvey, B.J., 2022. Do you CBI what I see? The relationship between the Composite Burn Index and quantitative field measures of burn severity varies across gradients of forest structure. Int. J. Wildl. Fire 31, 112–123. https://doi.org/10.1071/WF21062.

Schmitt, M., Hughes, L.H., Qiu, C., Zhu, X.X., 2019. Aggregating cloud-free Sentinel-2 images with Google Earth Engine. ISPRS Ann. Photogramm. Remote Sens. Spat. Inf. Sci. IV-2/W7, 145–152. https://doi.org/10.5194/isprs-annals-IV-2-W7-145-2019.

Sen, P.K., 1968. Estimates of the Regression Coefficient Based on Kendall's Tau. J. Am. Stat. Assoc. 63, 1379–1389. https://doi.org/10.2307/2285891.

Serbin, S.P., Ahl, D.E., Gower, S.T., 2013. Spatial and temporal validation of the MODIS LAI and FPAR products across a boreal forest wildfire chronosequence. Remote Sens. Environ. 133, 71–84. https://doi.org/10.1016/j.rse.2013.01.022.

Serrano-Notivoli, R., Saz, M.Á., Longares, L.A., de Luis, M., 2024. SiCLIMA: High-resolution hydroclimate and temperature dataset for Aragón (northeast Spain). Data Br. 56, 110876. https://doi.org/10.1016/j.dib.2024.110876.

Shakesby, R.A., Doerr, S.H., 2006. Wildfire as a hydrological and geomorphological agent. EarthSci. Rev. 74, 269–307. https://doi.org/10.1016/j.earscirev.2005.10.006.

Shi, M., McDowell, N., Huang, H., Zahura, F., Li, L., Chen, X., 2025. Ecosystem leaf area, gross primary production, and evapotranspiration responses to wildfire in the Columbia River Basin. Biogeosciences 22, 2225–2238. https://doi.org/10.5194/bg-22-2225-2025.

Smith-Tripp, S., Coops, N.C., Mulverhill, C., White, J., Gergel, S., 2026. Post-fire structural forest recovery associated with climate extremes in dry sub-boreal forests. Landsc. Ecol. 41, 14. https://doi.org/10.1007/s10980-025-02266-y.

Solans Vila, J.P., Barbosa, P., 2010. Post-fire vegetation regrowth detection in the Deiva Marina region (Liguria-Italy) using Landsat TM and ETM+ data. Ecol. Model. 221, 75–84. https://doi.org/10.1016/j.ecolmodel.2009.03.011.

Sousa, W.P., 1984. The role of disturbance in natural communities. Annu. Rev. Ecol. Syst. 15, 353–391. http://www.jstor.org/stable/2096953.

Stevens-Rumann, C.S., Morgan, P., 2019. Tree regeneration following wildfires in the western US: a review. Fire Ecol. 15, 1–17. https://doi.org/10.1186/s42408-019-0032-1.

Storey, E.A., Stow, D.A., Roberts, D.A., O'Leary, J.F., Davis, F.W., 2021. Evaluating Drought Impact on Postfire Recovery of Chaparral Across Southern California. Ecosystems 24, 806–824. https://doi.org/10.1007/s10021-020-00551-2.

Tappeiner, J.C.I.I., McDonald, P.M., Newton, M., Harrington, T.B., 1992. Ecology of hardwoods, shrubs, and herbaceous vegetation: effects on conifer regeneration. In: Hobbs, Tesch, S.D., Owston, S.D., others, P.W. (Eds.), Reforestation Practices in Southwestern Oregon and Northern California. Oregon State University, Forest Research Laboratory, Corvallis, OR, pp. 136–164.

Tárrega, R., Luis-Calabuig, E., Valbuena, L., 2001. Eleven years of recovery dynamic after experimental burning and cutting in two Cistus communities. Acta Oecologica 22, 277–283. https://doi.org/10.1016/S1146-609X(01)01125-0.

Tramblay, Y., Koutroulis, A., Samaniego, L., Vicente-Serrano, S.M., Volaire, F., Boone, A., Le Page, M., Llasat, M.C., Albergel, C., Burak, S., Cailleret, M., Kalin, K.C., Davi, H., Dupuy, J.-L., Greve, P., Grillakis, M., Hanich, L., Jarlan, L., Martin-StPaul, N., Martínez-Vilalta, J., Mouillot, F., Pulido-Velazquez, D., Quintana-Seguí, P., Renard, D., Turco, M., Türkeş, M., Trigo, R., Vidal, J.-P., Vilagrosa, A., Zribi, M., Polcher, J., 2020. Challenges for drought assessment in the Mediterranean region under future climate scenarios. EarthSci. Rev. 210, 103348. https://doi.org/10.1016/j.earscirev.2020.103348.

Van Wagtendonk, J.W., Root, R.R., Key, C.H., 2004. Comparison of AVIRIS and Landsat ETM+ detection capabilities for burn severity. Remote Sens. Environ. 92, 397–408. https://doi.org/10.1016/j.rse.2003.12.015.

Viana-Soto, A., Aguado, I., Salas, J., García, M., 2020. Identifying post-fire recovery trajectories and driving factors using landsat time series in fire-prone mediterranean pine forests. Remote Sens 12. https://doi.org/10.3390/RS12091499.

Vicente-Serrano, S.M., Beguería, S., López-Moreno, J.I., 2010. A multiscalar drought index sensitive to global warming: the standardized precipitation evapotranspiration index. J. Clim. 23, 1696–1718.

Vicente-Serrano, S.M., Pérez-Cabello, F., Lasanta, T., 2011. Pinus halepensis regeneration after a wildfire in a semiarid environment: assessment using multitemporal Landsat images. Int. J. Wildl. Fire 20, 195–208. https://doi.org/10.1071/WF08203.

Vicente-Serrano, S.M., Tomas-Burguera, M., Beguería, S., Reig, F., Latorre, B., Peña-Gallardo, M., Luna, M.Y., Morata, A., González-Hidalgo, J.C., 2017. A high resolution dataset of drought indices for Spain. Data 2, 22.

Vlassova, L., Pérez-Cabello, F., 2016. Effects of post-fire wood management strategies on vegetation recovery and land surface temperature (LST) estimated from Landsat images. Int. J. Appl. Earth Obs. Geoinf. 44, 171–183. https://doi.org/10.1016/j.jag.2015.08.011.

Volkova, L., Di Stefano, J., Thompson, E.K., Weston, C.J., 2025a. Influence of wildfire severity on plant and bird species richness, diversity and composition. Discov. Conserv 2 (1). https://doi.org/10.1007/s44353-024-00016-w.

Volkova, L., Paul, K.I., Roxburgh, S.H., Weston, C.J., 2025b. Recovery of south-eastern Australian temperate forest carbon is influenced by post-fire drought as well as fire severity. For. Ecol. Manag. 585, 122666. https://doi.org/10.1016/j.foreco.2025.122666.

Wang, J., Xiao, X., Bajgain, R., Starks, P., Steiner, J., Doughty, R.B., Chang, Q., 2019. Estimating leaf area index and aboveground biomass of grazing pastures using Sentinel-1, Sentinel-2 and Landsat images. ISPRS J. Photogramm. Remote Sens 154, 189–201. https://doi.org/10.1016/j.isprsjprs.2019.06.007.

Woodgate, W., Phinn, S., Devereux, T., Aryal, R.R., 2025. Bushfire recovery at a long-term tall eucalypt flux site through the lens of a satellite: Combining multi-scale data for structural-functional insight. Remote Sens. Environ. 317, 114530. https://doi.org/10.1016/j.rse.2024.114530.

Yan, K., Park, T., Yan, G., Chen, C., Yang, B., Liu, Z., Nemani, R.R., Knyazikhin, Y., Myneni, R.B., 2016. Evaluation of MODIS LAI/FPAR product collection 6. Part 1: Consistency and improvements. Remote Sens 8, 359. https://doi.org/10.3390/rs8050359.

Zang, J., Qiu, F., Zhang, Y., Shang, R., Liang, Y., 2025. A dataset of forest regrowth in globally key deforestation regions. Sci. Data 12, 154. https://doi.org/10.1038/s41597-025-04481-3.

Zhu, Z., Zhang, J., Yang, Z., Aljaddani, A.H., Cohen, W.B., Qiu, S., Zhou, C., 2020. Continuous monitoring of land disturbance based on Landsat time series. Remote Sens. Environ. 244, 111116. https://doi.org/10.1016/j.rse.2020.111824.